The Air Force Research Laboratory, Additive Manufacturing (AM) Modeling Challenge Series

Challenge Problem 4:

Microscale Structure -to- Properties

Released August 2019

Integrity ★ Service ★ Excellence

Table of Contents

General Problem Statement

Given an explicit microstructure representation and aggregate stress-strain behavior, predict grain-average elastic strain tensors for specified grains at specified macroscopic loading points under uniaxial tensile loading.

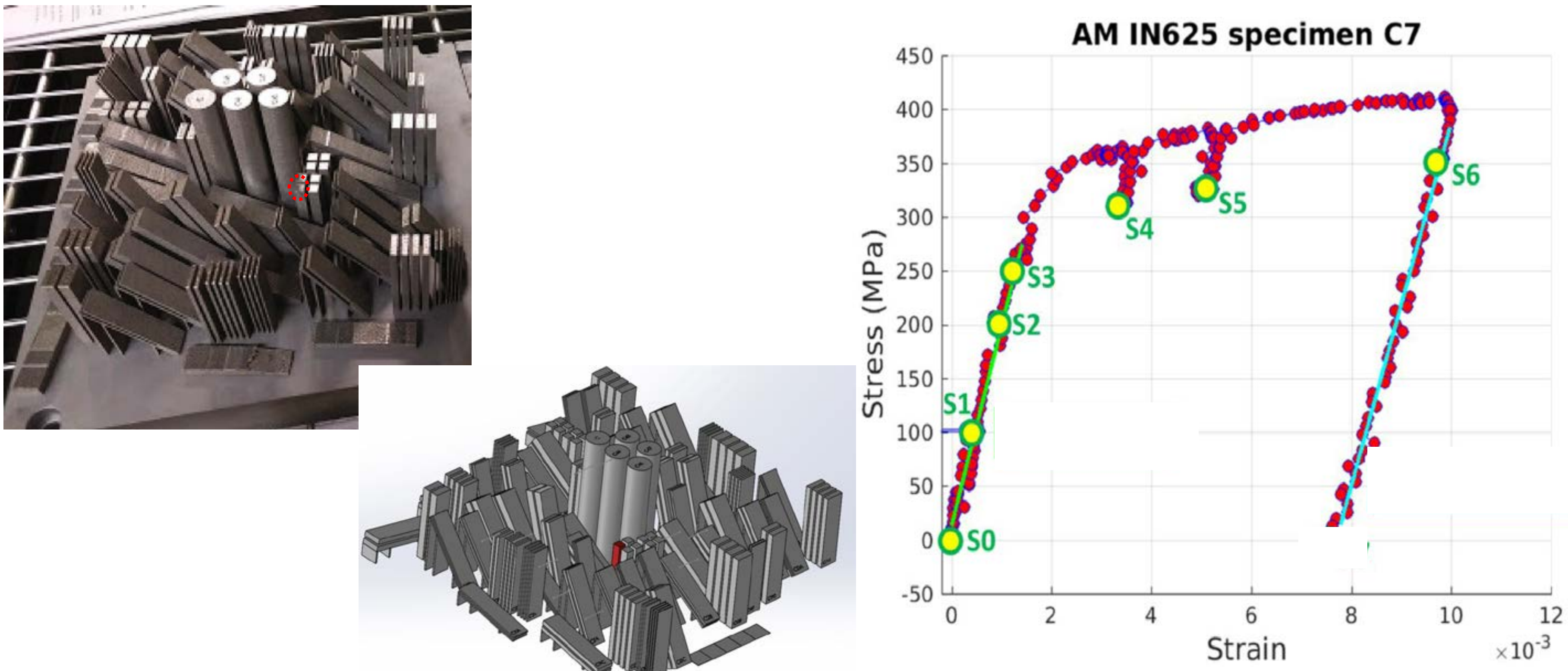

Fig. 1: Full build layout with the prism used for the HEDM sample (C7) highlighted in red and stress-strain curve with labeled macroscopic loading states where in situ characterization was performed

- Full build .stl file located in \Challenge4\CalibrationData\BuildGeometry

General Process Overview

- Samples were printed on an EOS M280 in 2017
  - EOS M280 is a Laser Powder Bed Fusion system (LPBF)
- Commercially available IN625 gas atomized powder was used as stock (slide 15 for material data provided by suppler)
- Using nominal processing parameters, a 5x5x35mm sample was printed with tensile/ long axis along build direction
- Sample went through a stress relief (SR) heat treatment, hot isostatic press (HIP) and heat treatment (HT). Referred to as SR+HIP+HT condition
- The sample was fully machined by wire electrical discharge machining (EDM). No further surface treatments/ machining was performed

(a) 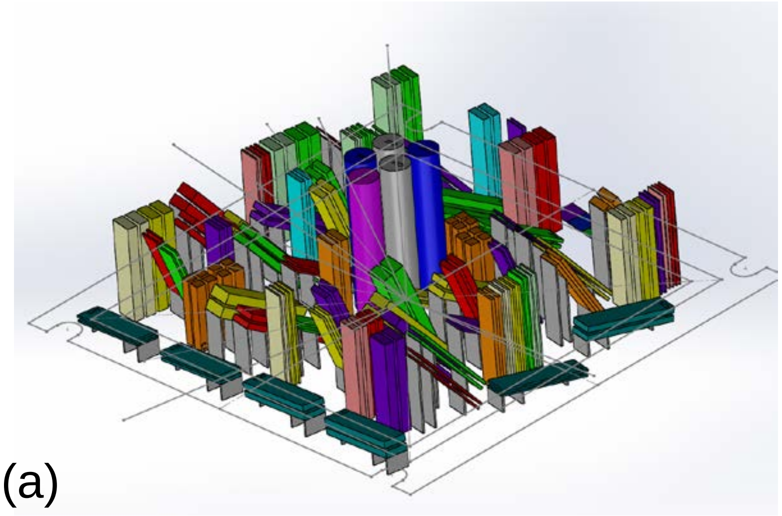

(b) 

(c) 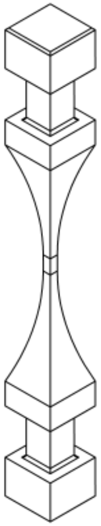

Fig. 2: (a)Schematic of the build plate, (b) photograph of full build plate and (c) schematic of the fully machined tensile sample

Overview of Characterization

- Gold fiducial markers were attached to the sample surface for tracking and alignment purposes.
- The sample was characterized using high energy diffraction microscopy (HEDM) techniques[1] (slide 7) at the Advanced Photon Source 1-ID-E beamline, located at Argonne National Laboratory. An *in situ* tensile test was conducted using the AFRL RAMS3 load frame[2] in conjunction with HEDM data collection. The sample was loaded to approximately 1% total strain, and grain average strains were measured for 7 macroscopic loading states along the stress strain curve as shown in slide 20.
- After tensile testing, regions of interest were 3D serial sectioned with electron backscatter diffraction (EBSD), backscattered electrons (BSE) and optical data collected throughout the volume (slide 10) using the AFRL LEROY system.
- The serial sectioned and HEDM data were registered and used to define the problem statement and describe the initial state of the material. (slide 11)

1. Schuren JC, Shade PA, Bernier JV, Li SF, Blank B, Lind J, Kenesei P, Lienert U, Suter RM, Turner TJ, Dimiduk DM, Almer J. 2015. New opportunities for quantitative tracking of polycrystal responses in three dimensions. *Curr. Opin. Solid State Mater. Sci.* 19:235-244. https://doi.org/10.1016/j.cossms.2014.11.003
2. Shade PA, Blank B, Schuren JC, Turner TJ, Kenesei P, Goetze K, Suter RM, Bernier JV, Li SF, Lind J, Lienert U, Almer J. 2015. A rotational and axial motion system load frame insert for in situ high energy x-ray studies. *Rev. Sci. Instrum.* 86:093902. https://doi.org/10.1063/1.4927855

Background Information

Measurement Description: HEDM

High Energy Diffraction Microscopy (HEDM) Testing

- ***Integration** of* three synchrotron x-ray techniques with ***in situ*** loading

- Micro-computed tomography (μ-CT)
  - Structure of voids/cracks

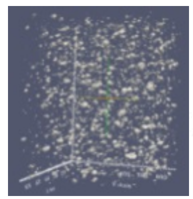

- Near field HEDM/3DXRD
  - 3D grain structure with sub-grain orientation resolution

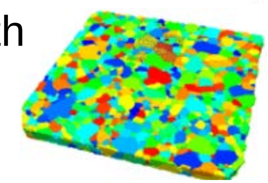

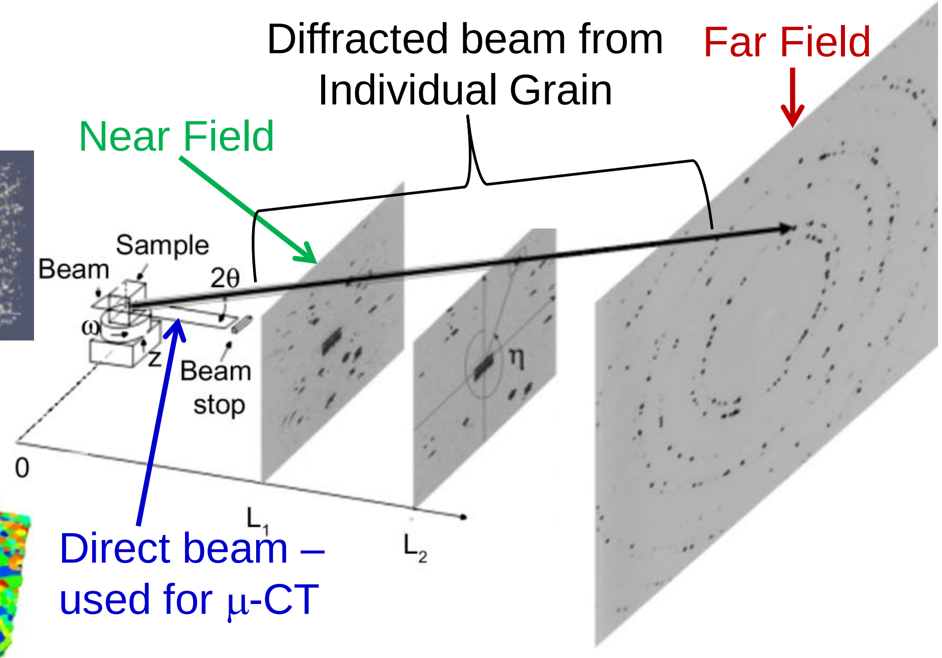

Adapted from: Poulsen HF. 2012. *J. Appl. Crystallogr.* 45:1084-1097

- Far field HEDM/3DXRD
  - Grain (or grain cross-section) resolved elastic strain tensors

$$\sigma_{ij} = C_{ijkl}\varepsilon_{kl}$$

Stress tensor with knowledge of elastic constants

Fig. 3: Schematic of the HEDM data collected before after and during uniaxial tensile loading of the sample

Measurement Description: HEDM

- Far field HEDM measurements provided grain-average elastic strain tensors
  - Gold fiducials were used to ensure consistent measurement alignment as well as help with subsequent dataset registration
  - 19 box beam layers, each 28.5 µm tall, were collected over a 541.5µm span in the center of a tensile specimen at each macroscopic loading point
  - Elastic strain tensors for grains that span multiple box beam layers were volume weighted by layer and the average strain tensors were calculated
- Micro-computed tomography and near field HEDM data were collected in the initial state to aid in dataset registration

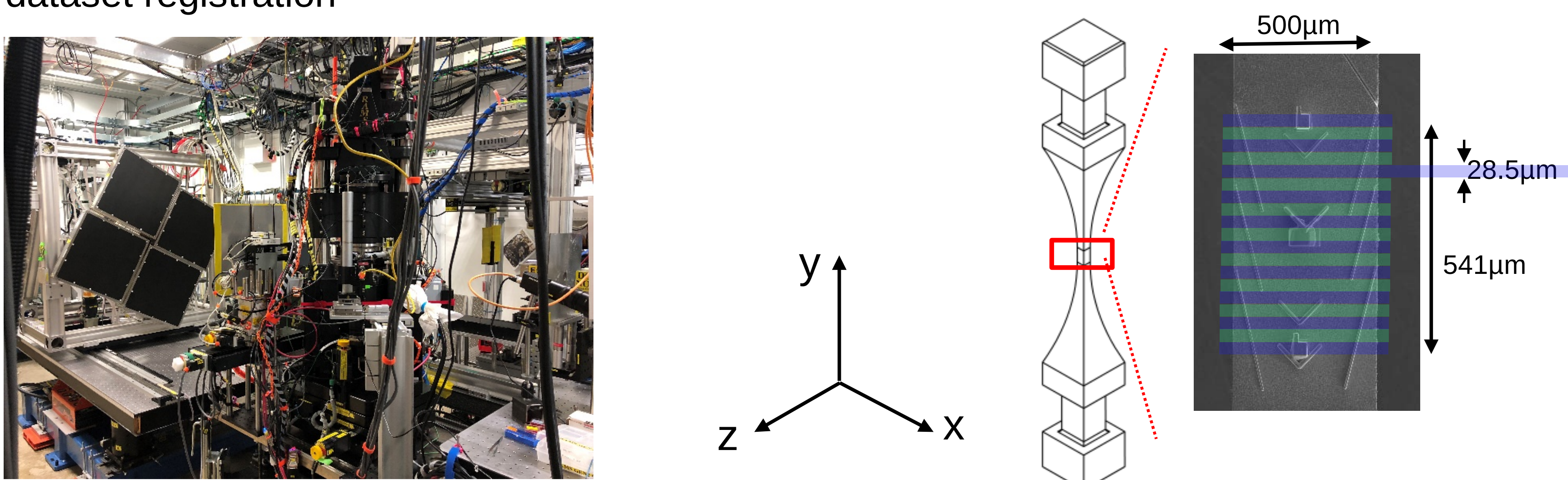

Fig. 4: Picture of experimental setup in APS 1-ID-E hutch and a schematic of the tensile specimen used in the challenge. Blue and green bands represent the box beam layers used to asses the material state during in situ characterization

Measurement Description: Tensile Testing with in situ HEDM

- The RAMS3 load frame developed by the Air Force / PulseRay and located at APS was utilized
- The tensile test was run in displacement control at a nominal strain rate of 10^{-4} s^{-1}
- Engineering strain was calculated using optical digital image correlation
- Loading was paused periodically to collect HEDM data

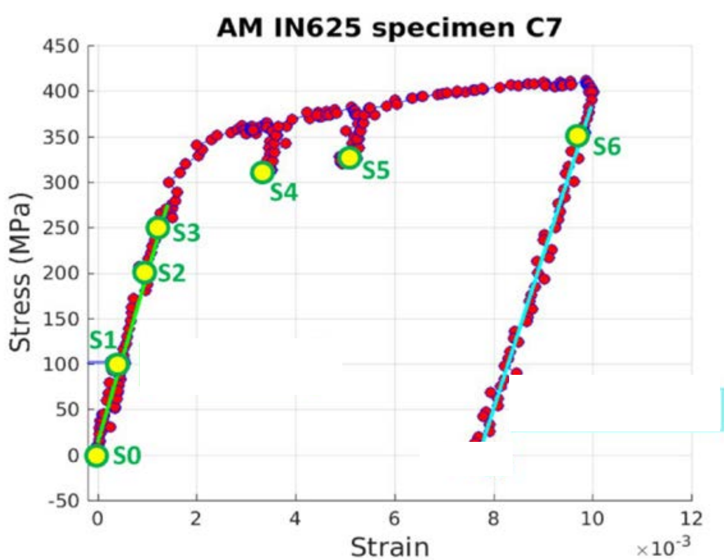

Fig. 5: Stress-strain curve with macroscopic loading states identified where the test was paused and HEDM measurements were collected

- In situ HEDM stress strain curve file located in \Challenge4\InputData

Measurement Description: Serial Sectioning

- Sample was 3D serial sectioned using the fully-automated LEROY system at AFRL/RXC, WPAFB[1]
  - Collected 3 data modes during destructive characterization (EBSD, BSE and OM)
  - 1000+ sections collected at approximately 1µm slice thickness
  - EBSD data were collected with 1µm step size in plane
- EBSD patterns were dictionary indexed[2] to assign crystallographic orientations

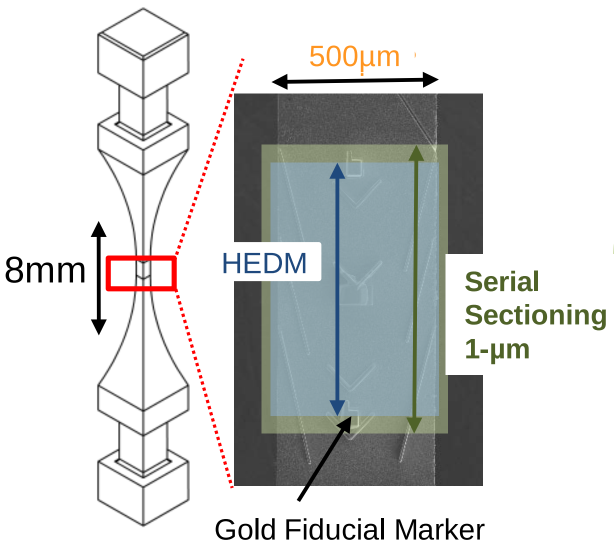

Fig. 6: Schematic of sample and areas that were serial sectioned

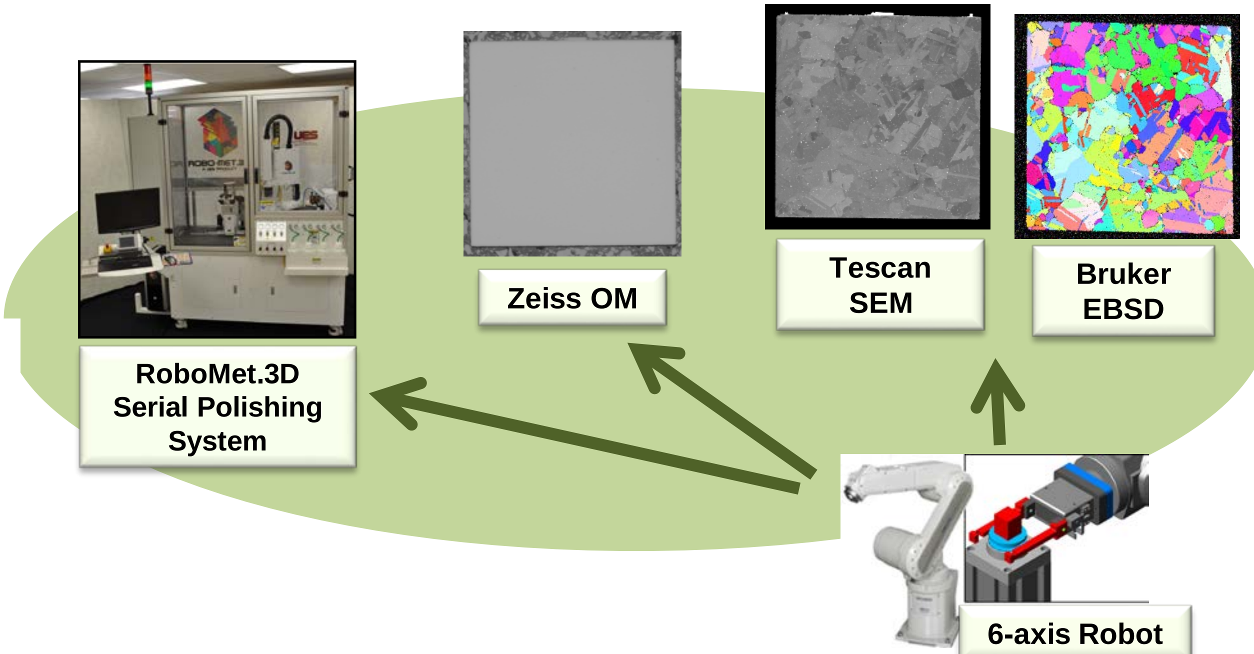

Fig. 7: Schematic of LEROY system modalities/stations

1. M. Uchic, M. Groeber, M. Shah, P. Callahan, A. Shiveley, M. Scott, M. Chapman, and J. Spowart "An Automated Multi-Modal Serial Sectioning System for Characterization of Grain Scale Microstructures in Engineering Materials," *Proceedings of the 1st International Conference on 3D Materials Science*, pp 195-202, 2012. https://doi.org/10.1007/978-3-319-48762-5_30
2. Y. H. Chen, S. U. Park, D. Wei, G. Newstadt, M. A. Jackson, J. P. Simmons, M. De Graef, and A. O. Hero, "A Dictionary Approach to Electron Backscatter Diffraction Indexing," *Microscopy and Microanalysis*, vol. 21, no. 3, pp. 739–752, 2015. doi:10.1017/S1431927615000756

Data Fusion: HEDM & Serial Sectioning

- Serial sectioning data were registered with the far field HEDM data to associate measured strain tensors with EBSD grains. The serial sectioning data are used to provide an approximation of the initial state microstructure and the far field HEDM data are used to provide grain average strain tensors.

<u>Assumptions</u>

- Microstructure morphology after 1% total strain (tensile loading) is representative of the microstructural morphology of the initial material state before loading.
- The grain average orientation was calculated and applied to the entire grain/feature as an approximation of the initial state.

<u>Challenge Grains</u>

- Grains that are identified with high confidence in far field HEDM across all loading states, are fully contained in the far field measurement region, and are uniquely correlated to grains from the 3D reconstructions (near field HEDM and serial sectioning) are used for the challenge question outlined later in the package.

Data for Model Calibration

Mechanical Testing

Tensile test data from calibration bars of AM IN625 with SR+HIP+HT post processing

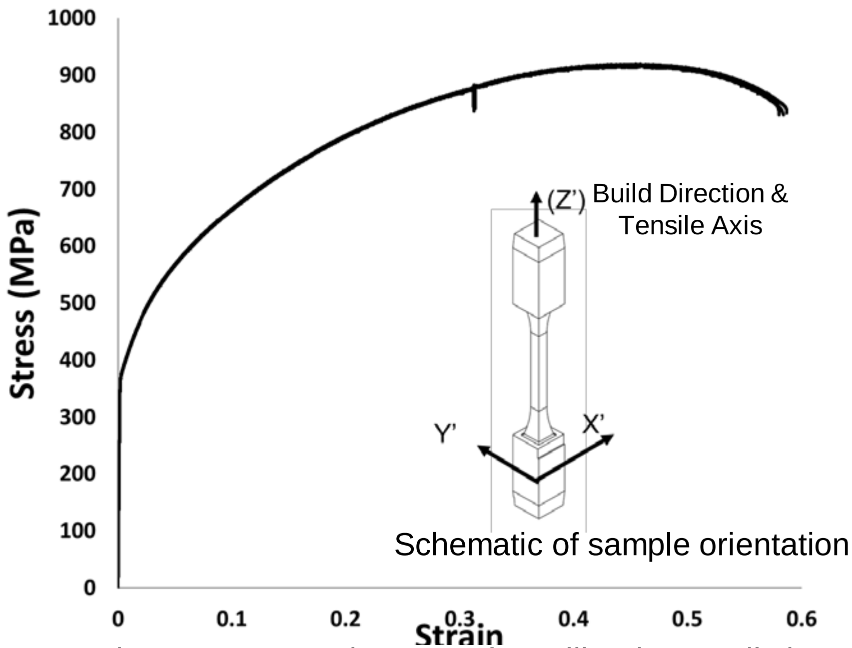

Fig. 8: Stress-strain curves for calibration tensile bar, designed using ASTM E8 as guidance, in SR+HIP+HT condition with schematic of sample orientation

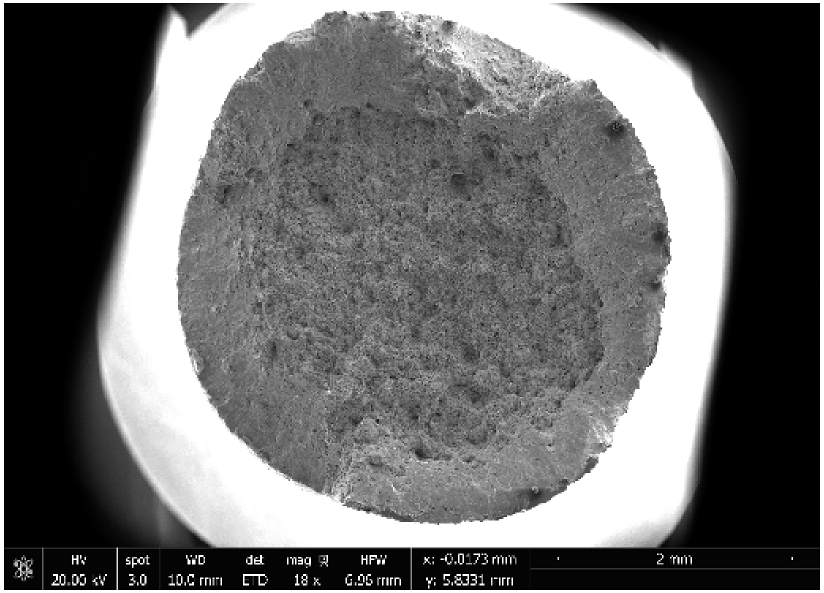

Fig. 9: Fracture surface images for calibration tensile bar SR+HIP+HT

Post Build Treatment	Build Angle	Sample Diameter [µm]	Test Temperature [ºF]	Elastic Modulus [GPa]	0.2% Yield Strength [MPa]	Stress @ 1%, 2%, 4%, 8%, 16% Strain [MPa]	Ultimate Tensile Strength [MPa]	Uniform Elongation
SR+HIP+HT	0	15	75	210.9	381.8	420.2, 470.1, 539.6, 629.5, 748.7	918.2	0.453

Table 1: Extracted mechanical properties for calibration tensile bars in SR+HIP+HT conditions at RT

- Raw stress-strain data for calibration tests located in \Challenge4\CalibrationData\MechanicalTestData
- Drawing of calibration tensile sample dimensions located in \Challenge4\Calibration Data\Mechanical TestData\Sample Geometry Details

Data for Model Calibration

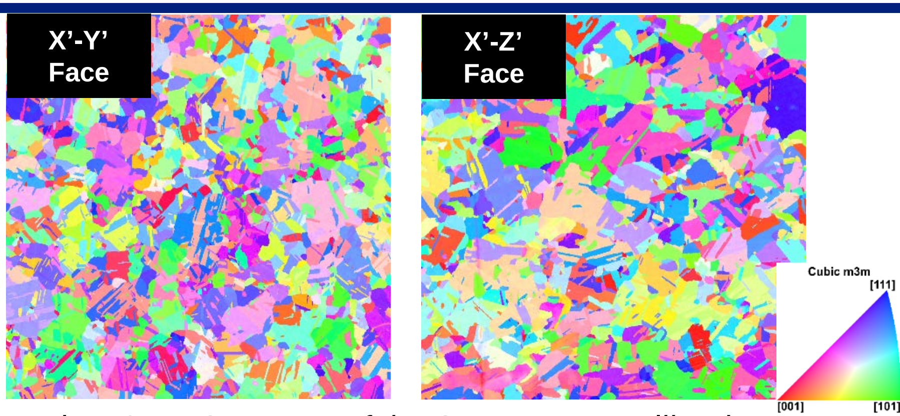

Fig. 10: EBSD scans of the SR+HIP+HT calibration cylinder. Each IPFZ map has a 1mm x 1mm field of view.

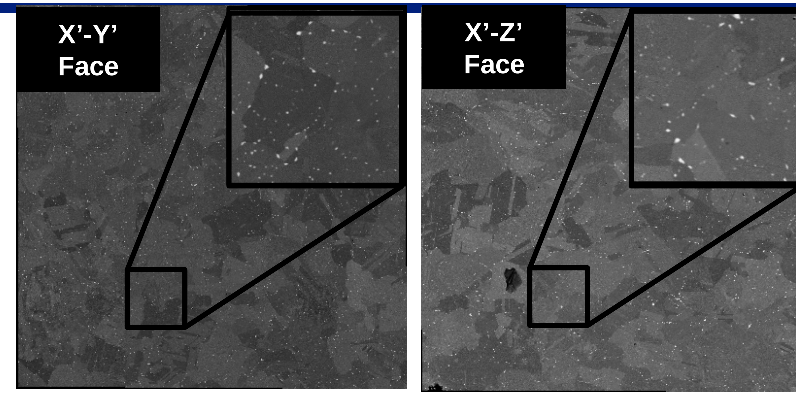

Fig. 11: BSE images of SR+HIP+HT calibration cylinder. Each image has approximately a 600x600µm field of view.

Twins Merged	X-Y Grain Size [µm] µ, σ	X-Y Aspect Ratio [µm] µ, σ	X-Z Grain Size [µm] µ, σ	X-Z Aspect Ratio [µm] µ, σ
No	17.1, 15.9	0.49, 0.20	15.6, 14.1	0.49, 0.19
Yes	22.5, 29.1	0.58, 0.18	18.4, 17.2	0.50, 0.19

Table 2: Grain statistics for calibration cylinder in SR+HIP+HT condition

Denuded Zone Thickness [µm]	X-Y Precipitate Size [µm] µ, σ	X-Y Precipitate V_f [%]	X-Z Precipitate Size [µm] µ, σ	X-Z Precipitate V_f [%]
N/A	0.94, 0.48	1.22	0.96, 0.53	1.19

Table 3: Precipitate statistics for calibration cylinder in SR+HIP+HT condition. See note on slide 30 (supplemental data).

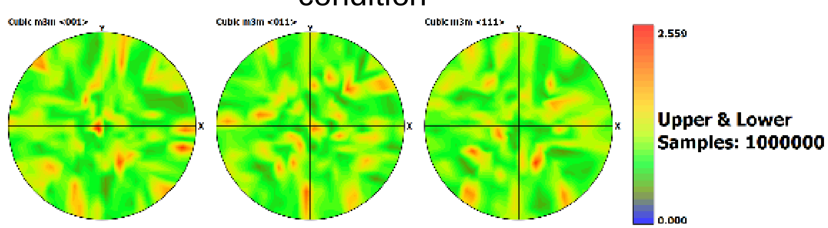

Fig. 12: Crystallographic orientation data for calibration cylinder in SR+HIP+HT condition

X-Y Void Size [µm] µ, σ	X-Y Void V_f %	X-Y R_a [µm]	X-Z Void Size [µm] µ, σ	X-Z Void V_f %	X-Z R_a [µm]
2.87, 3.79	0.016	< 1	2.79, 2.82	0.0159	< 1

Table 4: Void statistics for calibration cylinder & roughness statistics for the tensile bar in SR+HIP+HT condition

- Tabulated precipitate statistics located in \Challenge4\CalibrationData\MicrostructureData
- Raw BSE images located in \Challenge4\CalibrationData\MicrostructureData\BSE
- Tabulated grain statistics for calibration cylinders located in \Challenge4\CalibrationData\MicrostructureData
- Raw EBSD scans located in \Challenge4\CalibrationData\MicrostructureData\EBSD
- Analysis pipelines are located in \Challenge4\CalibrationData\Pipelines
- Discrete list of orientations can be extracted from the raw .ctf files in \Challenge4\CalibrationData\MicrostructureData\EBSD

Data for Model Calibration

Chemical Analysis (% wt)								
C	**Si**	**Mn**	**P**	**S**	**Cr**	**Ni**	**Mo**	**CbTa**
0.03 0.01	<0.01 0.05	<0.01 <0.01	<0.004 <0.001	0.002 <0.01	21.20 21.69	Bal Bal	8.91 9.06	3.56 3.75
Ti	**Al**	**B**	**Co**	**Cu**	**Fe**	**N**	**O**	**Ta**
0.01 0.02	0.05 0.04	0.001 0.001	<0.01 <0.01	0.01 0.01	3.09 2.12	0.008 0.005	0.015 0.035	<0.01 <0.02
Mg								
<0.001 <0.001								

Table 5: Chemical Analysis of IN625 Powder (prior to build)

- Chemical analysis of powder lot used in builds of single tracks and 2D pads
- Chemical analysis performed by powder supplier
- Gas atomized powder
- No post-build chemical analysis performed

Input Data for Challenge Question

Material Representation at Initial State

Initial Material State

- Sample was processed as described on slide 4 (AM In625 sample in SR+HIP+HT condition)
- 3D representation of the grain morphologies, grain averaged crystallographic orientations, and grain averaged strain tensors for S0 provided in the form of a DREAM.3D file.

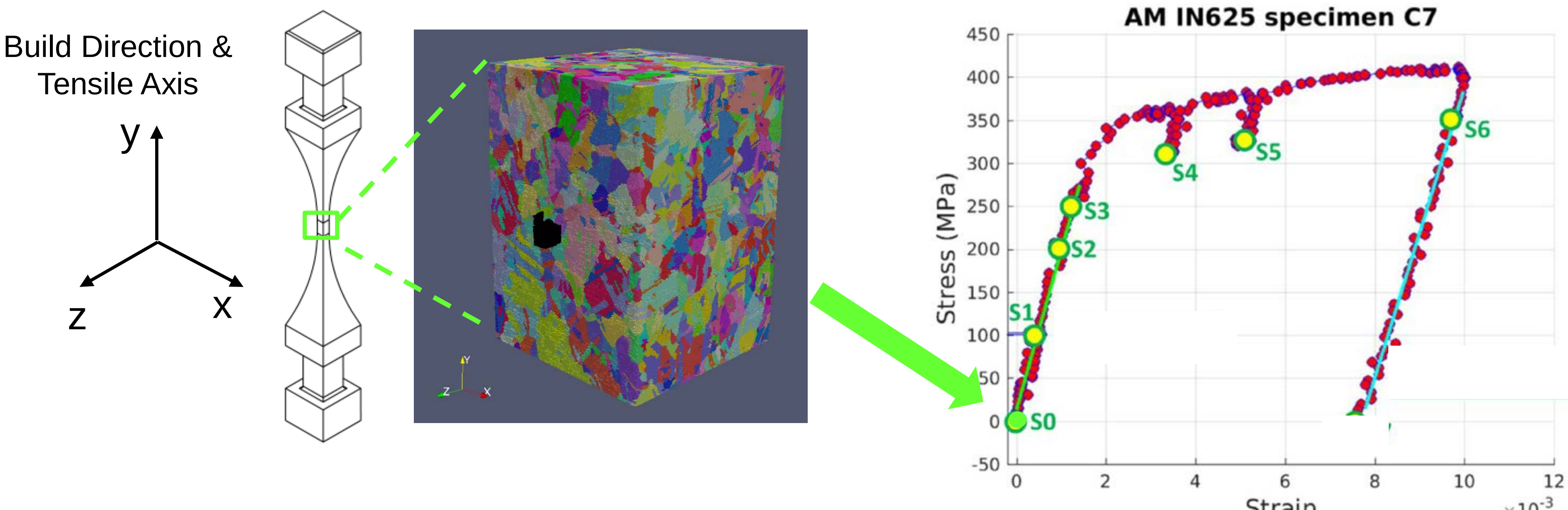

Fig. 13: 3D representation of assumed initial material state before sample deformation, S0 (macroscopic loading state 0)

- DREAM.3D file of the 3D representation of the initial material state located in \Challenge4\InputData

Challenge Data: Initial Conditions

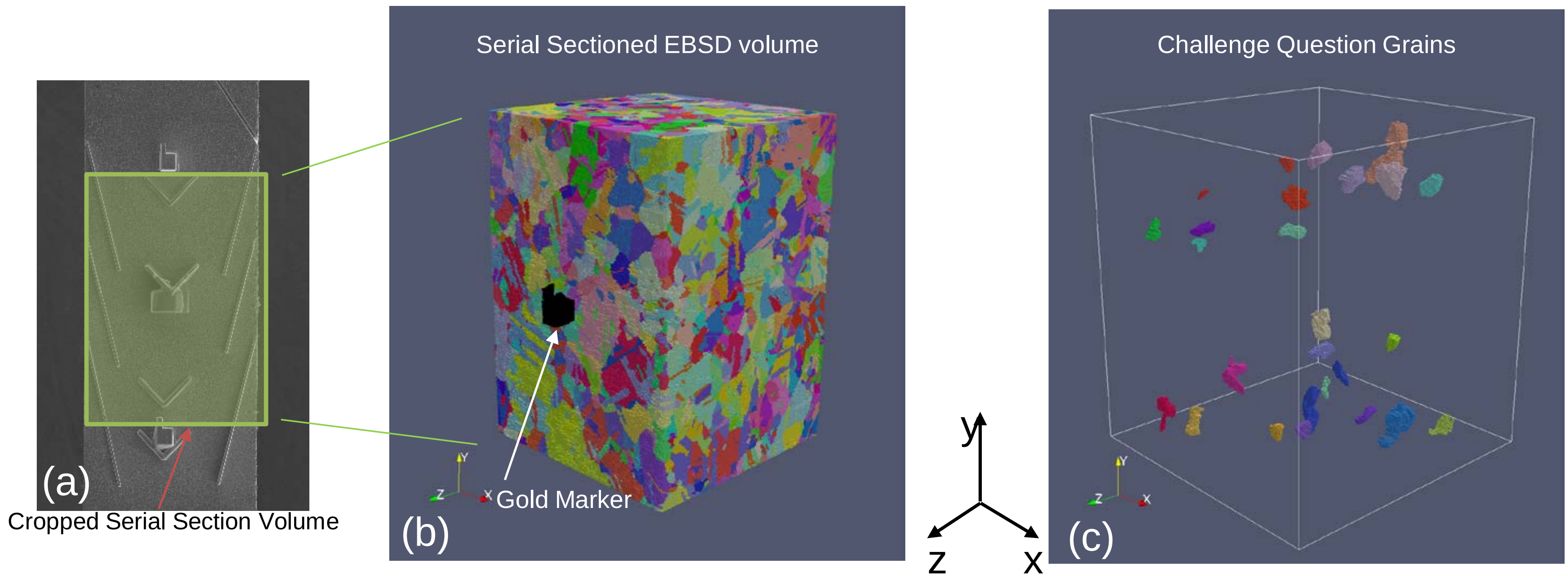

Fig. 14: (a) Imaging identifying the cropped serial section volume. 3D representations of assumed initial material state before sample deformation, S0 of (b) cropped serial section volume and (c) grains identified as challenge question grains

- Serial sectioning data and strain measurements are in same reference frame
- Y is the loading axis and the serial sectioning direction
- Serial sectioning volume was cropped right below and above top and bottom gold markers
- Resolution was down-sampled to 2µm in X, Y and Z
- Observed precipitates (~ 1 $\pm$ 0.5 µm , 1.2% Volume fraction) are not represented (see slides 29 & 30)
- Challenge Grains are identified in the provided DREAM.3D file

The Data File

- Filename = IN625InitialConditions.dream3d and IN625InitialConditions.xdmf
- Can be read into DREAM.3D: http://dream3d.bluequartz.net/
- Can be visualized with Paraview: https://www.paraview.org/
- HDF5 File Format: https://www.hdfgroup.org/solutions/hdf5/
- Data included:
  - Feature/Grain IDs
  - Phase Numbers
  - Average Euler Angles
  - Initial Strain States (averaged over the grain).
- More detailed information about the data file can be found in DREAM.3D_Data_Details.pptx file

- DREAM.3D data details power point is located in \Challenge4\InputData

Tensile Test Data

- The tensile test was run in displacement control at a nominal strain rate of 10^{-4} s^{-1}
- Engineering strain was calculated using optical digital image correlation
- Test was performed at room temperature (lab air)

Macroscopic loading states of HEDM measurements

- S0 = Initial unloaded state
- S1 = Load to 100 MPa and hold for measurement
- S2 = Load to 200 MPa and hold for measurement
- S3 = Load to 300 MPa, then unload by 50 MPa and hold for measurement
- S4 = Load to 0.35% total strain, then unload by 50 MPa and hold for measurement
- S5 = Load to 0.5% total strain, then unload by 50 MPa and hold for measurement
- S6 = Load to 1.0% total strain, then unload by 50 MPa and hold for measurement

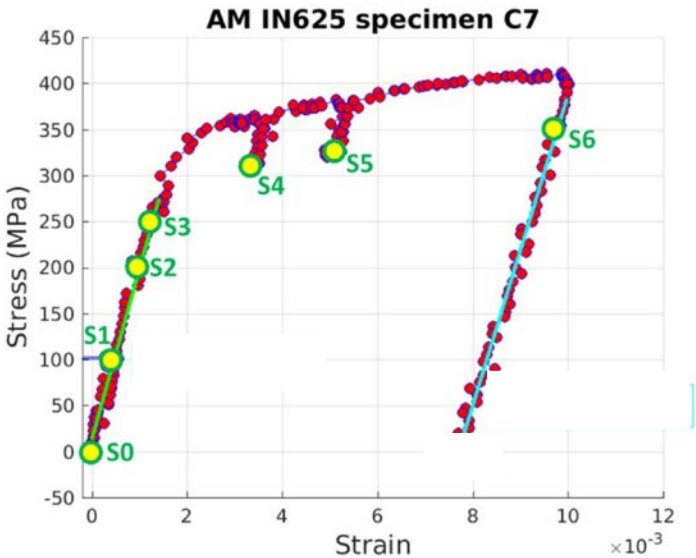

Fig. 15: Stress-strain curve with macroscopic loading states identified where the test was paused and HEDM measurements were collected

- In situ HEDM stress strain curve file located in \Challenge4\InputData

Challenge Question and Scoring

Challenge Question

- Given the initial material state, as defined in slide 17, predict strain tensor for each grain identified for macroscopic loading points S1-S6 (identified in slide 20).
  - Provide strain tensor in Voigt notation for each macroscopic loading point

Answer Format:

	Macroscopic Loading State 1 (S1)						Macroscopic Loading State (S2….S5)						Macroscopic Loading State (S6)					
Grain ID	ε_{xx}	ε_{yy}	ε_{zz}	ε_{yz}	ε_{xz}	ε_{xy}	ε_{xx}	ε_{yy}	ε_{zz}	ε_{yz}	ε_{xz}	ε_{xy}	ε_{xx}	ε_{yy}	ε_{zz}	ε_{yz}	ε_{xz}	ε_{xy}
18300																		
12602																		
7397																		
27757																		
19092																		
11766																		
21698																		
14655																		
25369																		
8445																		
12821																		
2489																		
145																		
317																		
5876																		
16576																		
15567																		
2841																		
15575																		
11248																		
19547																		
6191																		
1191																		
20330																		
12334																		
16504																		
3994																		
19571																		

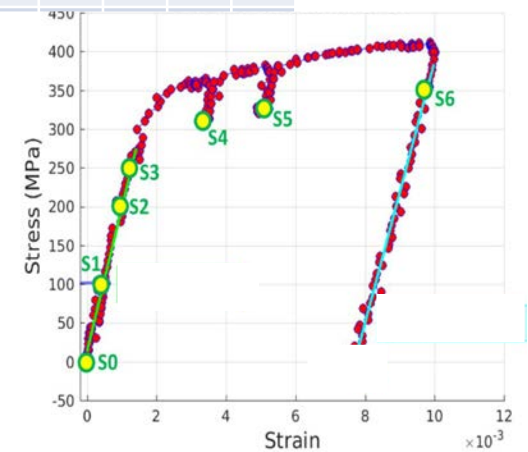

Table 6: Answer submission template

- Answer sheet template located in \Challenge4\Challenge 4 Answer Template.xls

Scoring

- Predictions for each grain at each macroscopic loading point are worth the same value
- An error will be calculated for each grain using L^2 norm
- Performers will be ranked based on the lowest cumulative error

- Responses must be returned within the document "Challenge 4 Answer Template.xlsx"
    - ***Answers returned in any other format will not be scored***

Supplemental Data

Single Crystal Modulus for Ni-based Superalloys
(From literature, non-AFRL data)

	Compliance (x10^{-3} [1/Gpa])			Stiffness [Gpa]			Anisotropy Ratio	
Material	S11	S12	S44	C11	C12	C44	C44/C'	Reference
IN625	-	-	-	243.3	156.7	117.8	2.72	[1]
IN600	-	-	-	234.6	145.4	126.2	2.83	[2]
*CMSX-4	8.02	-2.92	7.62	213.8	122.4	131.2	2.87	[3]
*CMSX-6	8.1	-2.96	7.82	213.2	122.8	127.9	2.83	[3]
*SRR99	7.95	-2.99	7.79	230.1	138.7	128.4	2.81	[3]
*IN738 LC	7.98	-3.08	7.71	243.4	153	129.7	2.87	[3]
SX Ni-base Superalloy	7.7	-2.9	7.1	238.33	143.99	140.85	2.99	[4]
IN718 - GFMA	-	-	-	242.18	138.85	104.2	2.02	[5]
Waspaloy	-	-	-	266.27	141.31	104.63	1.67	[5]
Pure Ni	-	-	-	250	160	118	2.62	[5]
In718 (FCC Matrix)	-	-	-	272.1	169	131	2.54	[6]
IN718	-	-	-	259.6	179	109.6	2.72	[7]
AM1	-	-	-	296	204	125	2.72	[8]

$$C_{11} = \frac{S_{11} + S_{12}}{(S_{11} - S_{12})(S_{11} + 2S_{12})} \qquad C' = \frac{C_{11} - C_{12}}{2}$$

$$C_{12} = \frac{-S_{12}}{(S_{11} - S_{12})(S_{11} + 2S_{12})} \qquad C_{44} = \frac{1}{S_{44}}$$

	C11	C12	C44	C44/C'
Min	213.2	122.4	104.2	1.67
Max	296	204	140.85	2.99
Avg	246.38	151.93	122.65	2.63
Std Dev	23.05	22.56	11.12	0.37

Table 7: Compiled single crystal modulus data compiled from the literature with reference

References:

[1] Z. Wang, A.D. Stoica, D. Ma, A.M. Beese (2016). Diffraction and single-crystal elastic constants of Inconel 625 at room and elevated temperatures determined by neutron diffraction. Mat Sci & Eng A, 674, 406-412. https://doi.org/10.1016/j.msea.2016.08.010

[2] T.M. Holden, R.A. Holt, A.P. Clarke (1998). Intergranular strains in Inconel-600 and the impact on interpreting stress fields in bent steam-generator tubing. Mat Sci & Eng A246, 180-198. https://doi.org/10.1016/S0921-5093(97)00732-6

[3] W. Hermann, H.G. Sockel, J. Han, A. Bertram (1996). Elastic properties and determination of elastic constants of nickel-base superalloys by a free-free beam technique. Superalloys 1996, TMS, 229-238. DOI: 10.7449/1996/Superalloys_1996_229_238

[4] S.W. Yang (1965), Elastic constants of a monocrystalline nickel-base superalloy, Met Trans A, 16A, 661-665. https://doi.org/10.1007/BF02814240

[5] P. Haldipur (2006), Material characterization of nickel-based super alloys through ultrasonic inspection, Retrospective Theses and Dissertations, Iowa State University. https://doi.org/10.31274/rtd-180813-12105

[6] S. Ghorbanpour et al. (2017), A crystal plasticity model incorporating the effects of precipitates in superalloys: Application to tensile, compressive, and cyclic deformation of Inconel 718, Int J Plast, 99, 162-185. https://doi.org/10.1016/j.ijplas.2017.09.006

[7] G. Martin et al. (2014), A multiscale model for the elastoviscoplastic behavior of directionally solidified alloys: Application to FE structural computations, Int J Solids & Struct, 51-5, 1175-1187. https://doi.org/10.1016/j.ijsolstr.2013.12.013

[8] F. Hanriot, G. Cailletaud, L. Remy (1991), Mechanical behavior of a nickel-base superalloy single crystal. In: Proc. Of Int. Symp. High Temperature Constitutive Modeling: Theory and Application, Georgia, Winter Annual Meeting, ASME.

*Estimated (S11, S12, S44) values from graphs showing compliance as a function of temperature. C11, C12, and C44 are calculated based on equations above.

Additional Mechanical Testing Data

Tensile test data from calibration tensile bars of AM IN625

NOTE: The challenge sample/question is in the SR+HIP+HT condition. SR Only condition provided but not an input condition to the challenge.

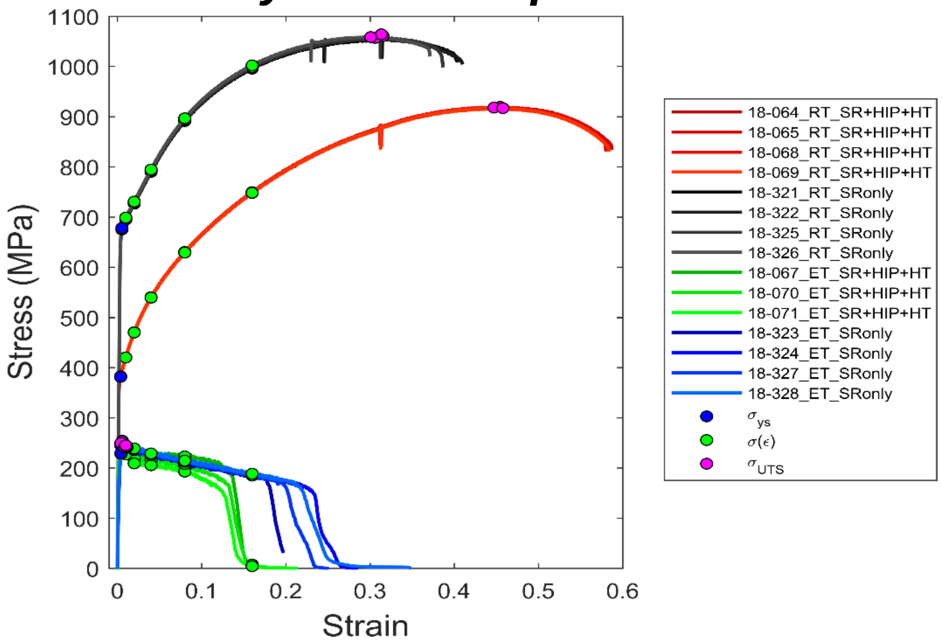

Fig. 16: Stress-strain curves for calibration tensile bars in SR Only (black=RT, blue=ET) and SR+HIP+HT (red=RT, green=ET) conditions

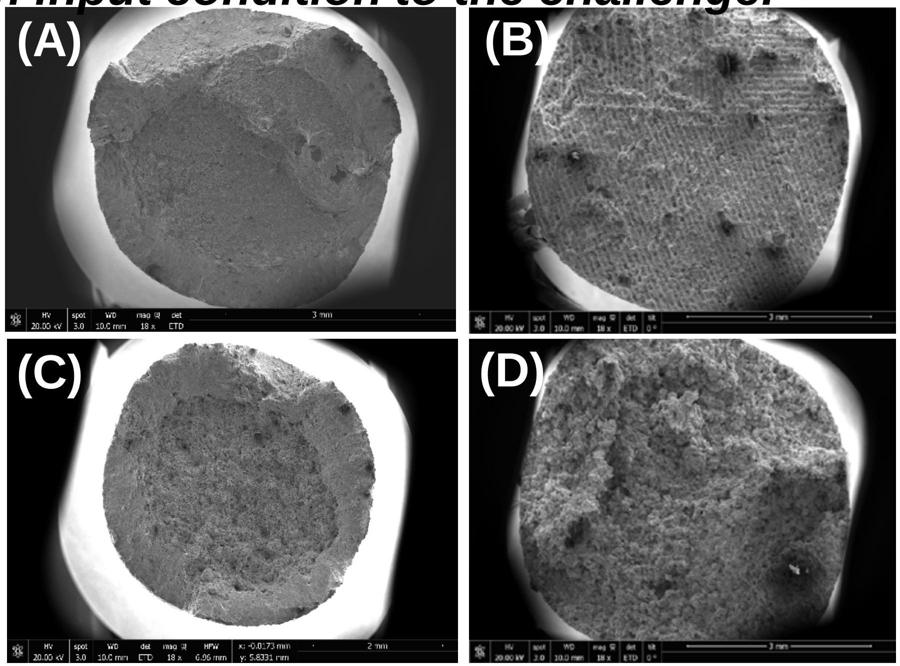

Fig. 17: Fracture surface images for calibration tensile bars (A) SR Only @ RT, (B) SR Only @ ET, (C) SR+HIP+HT @ RT and (D) SR+HIP+HT @ ET

Post Build Treatment	Build Angle	Sample Diameter [mm]	Test Temperature [ºF]	Elastic Modulus [GPa]	0.2% Yield Strength [MPa]	Stress @ 1%, 2%, 4%, 8%, 16% Strain [MPa]	Ultimate Tensile Strength [MPa]	Uniform Elongation
SR+HIP+HT	0	15	75	210.9	381.8	420.2, 470.1, 539.6, 629.5, 748.7	918.2	0.453
SR	0	15	75	197.8	676.7	697.0, 728.6, 792.2, 893.6, 998.5	1060.1	0.309
SR+HIP+HT	0	15	1600	128.6	247.3	235.8, 217.2, 216.3, 206.1, 5.6	252.1	0.0053
SR	0	15	1600	101.0	228.7	240.8, 236.8, 227.2, 211.7, 188.4	242.6	0.01

Table 8: Extracted mechanical properties for calibration tensile bars tensile bars in SR Only and SR+HIP+HT conditions at room temperature (RT) and elevated temperature (ET)

- Raw stress-strain data for calibration tests located in \Challenge4\SupplementalData\MechanicalTestData

Additional Material Characterization

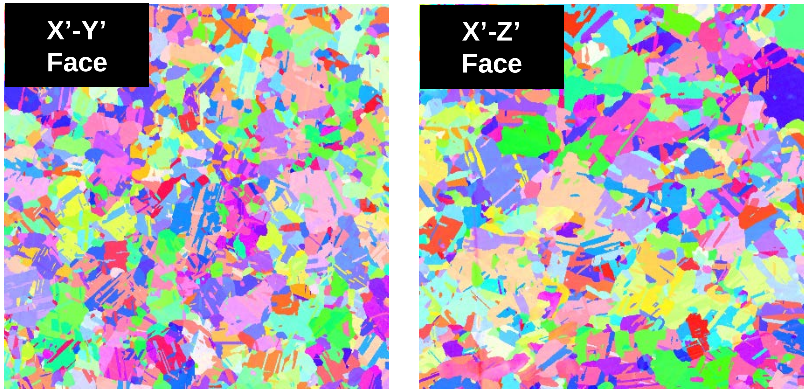

Fig. 18: EBSD scans of the SR+HIP+HT calibration cylinder. Each IPFZ map has a 1mm x 1mm field of view.

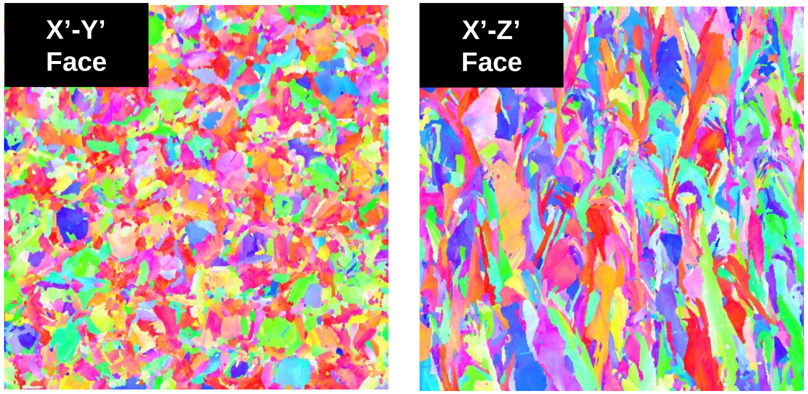

Fig. 19: EBSD scans of the SR Only calibration cylinder. Each IPFZ map has a 1mm x 1mm field of view.

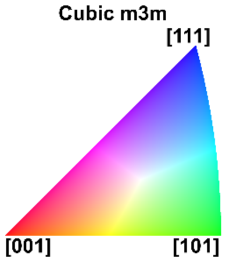

SR+HIP+HT

Twins Merged	X-Y Grain Size [µm] µ, σ	X-Y Aspect Ratio [µm] µ, σ	X-Z Grain Size [µm] µ, σ	X-Z Aspect Ratio [µm] µ, σ
No	17.1, 15.9	0.49, 0.20	15.6, 14.1	0.49, 0.19
Yes	22.5, 29.1	0.58, 0.18	18.4, 17.2	0.50, 0.19

Table 9: Grain statistics for cin SR+HIP+HT condition

SR Only

X-Y Grain Size [µm] µ, σ	X-Y Aspect Ratio [µm] µ, σ	X-Z Grain Size [µm] µ, σ	X-Z Aspect Ratio [µm] µ, σ
15.2, 12.7	0.56, 0.18	16.1, 15.7	0.41, 0.20

Table 10: Grain statistics for milli-tensile sample in SR Only condition

- Tabulated grain statistics for calibration bars located in \Challenge4\SupplementalData\MicrostructureData
- Raw EBSD scans located in \Challenge4\SupplementalData\MicrostructureData\EBSD
- Analysis pipelines are located in \Challenge4\CalibrationData\Pipelines

Additional Material Characterization

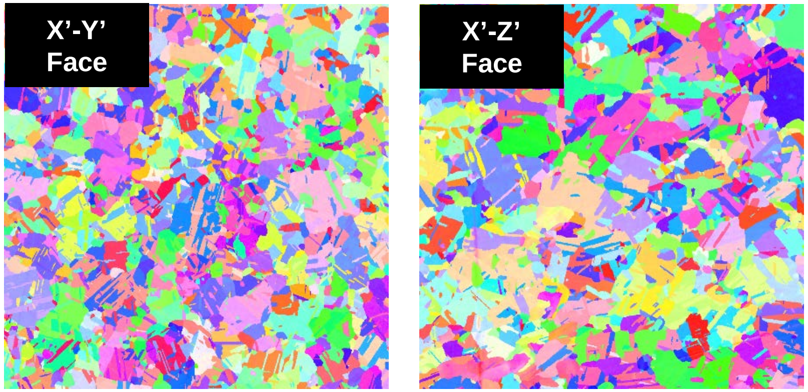

Fig. 18: EBSD scans of the SR+HIP+HT calibration cylinder. Each IPFZ map has a 1mm x 1mm field of view

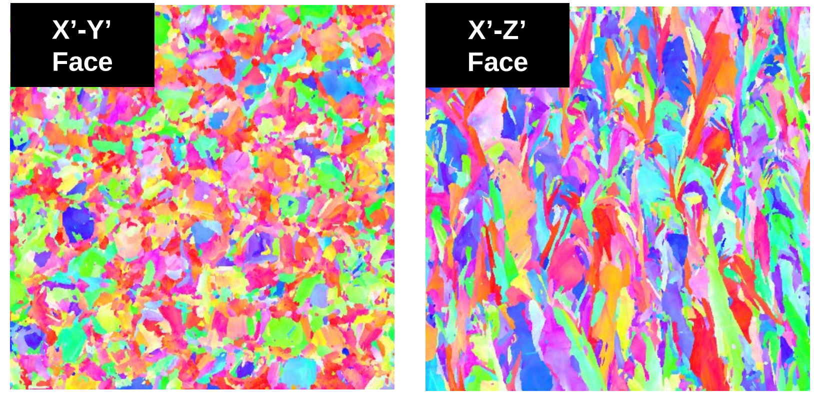

Fig. 19: EBSD scans of the SR Only calibration cylinder. Each IPFZ map has a 1mm x 1mm field of view

SR+HIP+HT

Build Angle	Thickness [µm]	Pole Figures
0	15	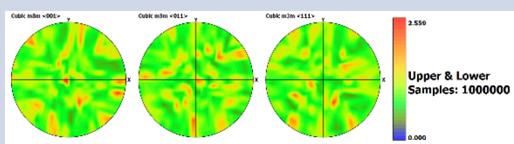

Table 11: Crystallographic orientation data for calibration cylinder in SR+HIP+HT condition

SR Only

Build Angle	Thickness [µm]	Pole Figures
0	15	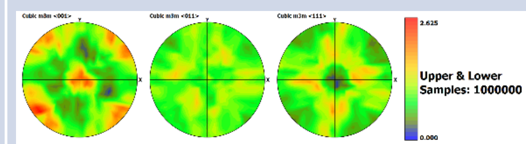

Table 12: Crystallographic orientation data for calibration cylinder in SR Only condition

- Discrete list of orientations can be extracted from the raw .ctf files in \Challenge4\SupplementalData\MicrostructureData\EBSD

Additional Material Characterization

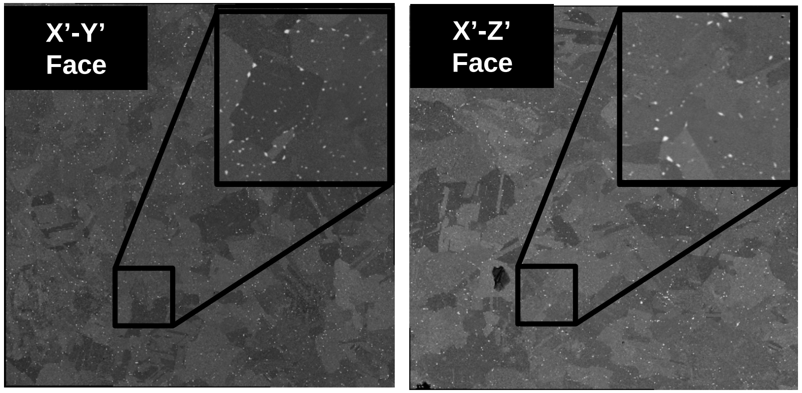

Fig. 20: BSE images of SR+HIP+HT calibration cylinder. Each image has approximately a 600x600µm field of view.

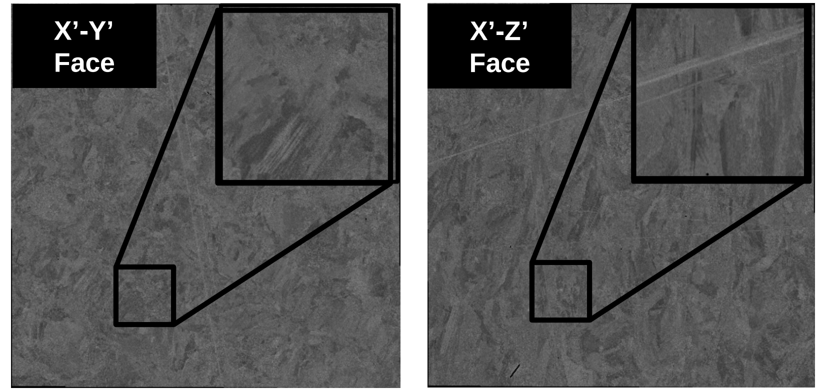

Fig. 21: BSE images of SR Only calibration cylinder. Each image has approximately a 600x600µm field of view.

SR+HIP+HT

Denuded Zone Thickness [µm]	X-Y Precipitate Size [µm] µ, σ	X-Y Precipitate V_f [%]	X-Z Precipitate Size [µm] µ, σ	X-Z Precipitate V_f [%]
N/A	0.94, 0.48	1.22	0.96, 0.53	1.19

Table 13: Precipitate statistics for calibration cylinder in SR+HIP+HT condition

SR Only

X-Y Precipitate Size [µm] µ, σ	X-Y Precipitate V_f [%]	X-Z Precipitate Size [µm] µ, σ	X-Z Precipitate V_f [%]
N/A	0	N/A	0

Table 14: Precipitate statistics for calibration cylinder in SR Only condition

- Tabulated precipitate statistics located in \Challenge4\SupplementalData\MicrostructureData
- Raw BSE images located in Challenge4\SupplementalData\MicrostructureData\BSE
- Analysis pipelines located in \Challenge3\Calibration\Pipelines

Additional Material Characterization

Volume fraction reported is likely underestimated slightly and average size is likely overestimated

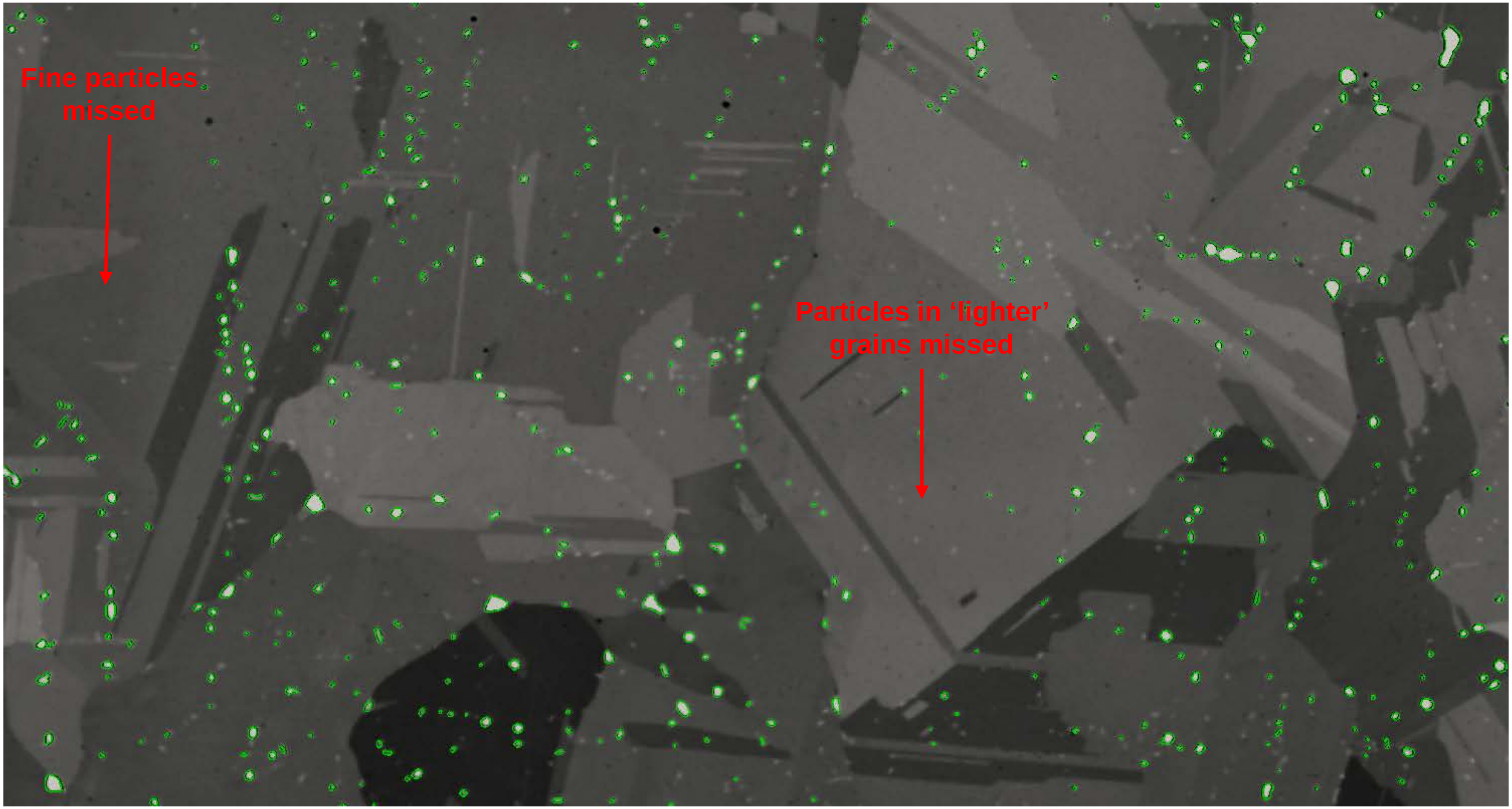

Fig. 15: Example segmentation of precipitates in BSE images of calibration cylinder with annotations showing missed particles.

* Note: area shown is approx. 1/10th of area used to calculate statistics for a given sample on a given plane *

- Analysis pipelines located in \Challenge4\Calibration\Pipelines